MRI-Guided Biopsy to Correlate Tissue Specimens with MR Elastography Stiffness Readings in Liver Transplants

Ryan B. Perumpail, BA[1], **Josh Levitsky, MD**[2], **Yi Wang, MD**[1], **Victoria S. Lee, BA**[2], **Jennifer Karp, BSN, RN**[1], **Ning Jin, MS**[1], **Guang-Yu Yang, MD, PhD**[3], **Bradley D. Bolster Jr, PhD**[4], **Saurabh Shah, MS**[5], **Sven Zuehlsdorff, PhD**[5], **Albert A. Nemcek Jr, MD**[1], **Andrew C. Larson, PhD**[1], **Frank H. Miller, MD**[1], and **Reed A. Omary, MD, MS**[1]

[1] Department of Radiology Northwestern University, Chicago, IL

[2] Department of Medicine, Northwestern University, Chicago, IL

[3] Department of Pathology Northwestern University, Chicago, IL

[4] Siemens Medical Solutions, Rochester, MN, Chicago, IL, USA

[5] Siemens Medical Solutions Chicago, IL, USA.

Abstract

Rationale and Objectives—Magnetic resonance elastography (MRE) can non-invasively measure the stiffness of liver tissue and display this information in anatomic maps. Magnetic resonance imaging (MRI)-guidance has not previously been used to biopsy segments of heterogeneous stiffness identified on MRE. Dedicated study of MRE in post-liver transplant patients is also limited. In this study, the ability of real-time MRI to guide biopsies of segments of the liver with different MRE stiffness values in the same post-transplant patient was assessed.

Materials and Methods—MRE was performed in 9 consecutive post-transplant patients with history of hepatitis C. Segments of highest and lower stiffness on MRE served as targets for subsequent real-time MRI-guided biopsy using T2-weighted imaging. The ability of MRI-guided biopsy to successfully obtain tissue specimens was assessed. The Wilcoxon Signed Rank Test was used to compare mean stiffness differences for highest and lower MRE stiffness segments, with $\alpha = 0.05$.

Results—MRI-guidance allowed successful sampling of liver tissue for all (18/18) biopsies. There was a statistically significant difference in mean MRE stiffness values between highest (4.61 ± 1.99 kPa) and lower stiffness (3.03 ± 1.75 kPa) (P=0.0039) segments biopsied in the 9 post-transplant patients.

Conclusion—Real-time MRI can guide biopsy in patients after liver transplantation based upon MRE stiffness values. This study supports the use of MRI-guidance to sample tissue based upon functional information.

Corresponding Author Reed A. Omary, MD, MS Department of Radiology, Northwestern University 737 N Michigan Ave, Suite 1600, Chicago, IL 60611, USA. reed@northwestern.edu Phone: (312) 695-3774 Fax: (312) 926-5991 .

Publisher's Disclaimer: This is a PDF file of an unedited manuscript that has been accepted for publication. As a service to our customers we are providing this early version of the manuscript. The manuscript will undergo copyediting, typesetting, and review of the resulting proof before it is published in its final citable form. Please note that during the production process errors may be discovered which could affect the content, and all legal disclaimers that apply to the journal pertain.

Conflicts of Interest Bolster BD Jr., Shah S, and Zuehlsdorff S are employed by Siemens Medical Solutions.

INTRODUCTION

Hepatitis C virus (HCV) infection afflicts an estimated 123 million people worldwide and is the leading indication for liver transplantation in the United States (1, 2). Post-transplant recurrence of HCV is virtually universal (2, 3). Although over 25% of HCV-positive patients develop fibrosis and ultimately cirrhosis within 5 years of transplant, it is unknown which specific patients will progress (2, 3). Post-transplant patients undergo recurrent liver biopsies because HCV therapy is reserved for biopsy-proven recurrence (4). Sampling error is a major limitation of biopsies due to the heterogeneity of early fibrosis and the small amount of tissue obtained per biopsy (0.002% of the overall liver volume) (5, 6). The use of imaging guidance to target the stiffest segments of liver is one potential solution to this limitation but requires a method that can simultaneously identify the local liver stiffness and guide needle placement.

Magnetic resonance imaging (MRI)-guidance can be used to biopsy liver lesions with diagnostic yields similar to computed tomography (CT) and ultrasound (US) guidance methods (7). MRI-guidance has not previously been used to biopsy focal segments of heterogeneous stiffness identified on magnetic resonance elastography (MRE). MRE, pioneered by Dr. Richard Ehman (8), has emerged as a powerful method to non-invasively measure the liver's stiffness, which in turn correlates with the presence of generalized liver fibrosis in patients with chronic liver disease (9). Such information is displayed as color-coded, quantitative stiffness maps. Because higher stiffness readings are associated with increased fibrosis, stiffness maps enable distinction between normal and fibrotic livers. A cutoff value of 2.93 kPa for mean liver stiffness is 98% sensitive and 99% specific to distinguish normal from fibrotic livers in patients without liver transplants (9). There is emerging data on MRE in post-transplant patients, a high-risk population that stands to benefit greatly from the technique (10). Furthermore, it is unclear whether MRI-guidance can be used to biopsy regions of heterogeneous liver stiffness seen in post-transplant patients.

In this study, the ability of real-time MRI to guide biopsies of separate segments of the liver in post-transplant patients with heterogeneous stiffness values was assessed. Validation of this ability would indicate that MRI can guide tissue sampling that correlates with functional imaging information, rather than its more common use for targeting tumors based upon traditional anatomic findings.

MATERIALS AND METHODS

Clinical Setting and Patients

This prospective Health Insurance Portability and Accountability Act-compliant study was approved by the local institutional review board. All patients provided informed consent. The study was performed at a single hospital over 3 consecutive months. The feasibility of combined MRE/MRI-guided liver biopsy was first validated in two patients (1 male, 1 female; age range, 46-60 years) without liver transplantation who were already scheduled for biopsy. Next, nine consecutive post-transplant patients (7 male, 2 female; age range, 42-65 years; mean age, 56 ± 6.4 years) were enrolled in this study for outpatient liver MRI/MRE followed by same-day real-time MRI-guided liver biopsies. All patients had

previously undergone liver transplantation due to complications of chronic HCV infection. The inclusion criteria for enrollment were a) history of liver transplantation, b) ability to undergo MRI, and c) informed consent. Exclusion criteria were a) age younger than 18 years, b) inability to provide informed consent, c) uncorrectable thrombocytopenia (platelet count < 50,000/μL), d) uncorrectable coagulopathy (international normalized ratio > 1.5), or e) contraindications to MRI.

MRI Unit

Diagnostic MRI (including MRE) and MRI-guided biopsies were both performed in the medical center's interventional MRI procedure suite using a 1.5-T Espree MRI scanner (Siemens, Erlangen, Germany).

Magnetic Resonance Elastography

Conventional anatomic MRI of the liver included axial and coronal T2-weighted half-Fourier acquisition single-shot turbo spin-echo (HASTE), axial T1-weighted in-phase and out-of-phase gradient recalled echo, T2-weighted turbo spin-echo with fat suppression, and T1-weighted fat-suppressed gradient-echo using shared prepulses.

Following conventional MRI, all patients underwent MRE using a 19-cm diameter cylindrical acoustic driver to generate 60 Hz mechanical vibrations overlying the liver. The propagating shear waves were imaged with a modified phase-contrast gradient-echo sequence with parameters as follows: repetition time/echo time/flip angle, 100 ms/24.2 ms/ 15°; field of view, 390×390 mm^2; acquisition matrix, 256×64; slice thickness, 5 mm; bandwidth, 260 Hz/pixel; imaging frequency, 63.5 MHz; scan time, 29 seconds per image. The acquired images were processed with a previously described direct inversion algorithm to generate quantitative images of shear stiffness (MR elastograms) (9, 11).

Magnetic Resonance Elastography Analysis

Using MRE scans, an attending radiologist first identified the Couinaud segment of highest stiffness and one segment of lower stiffness as targets for MRI-guided biopsy for each patient and then measured MRE stiffness values for each of these focal areas. The overall MRE stiffness for each liver was also measured by selecting and averaging the stiffness values for two to three 200 mm^2 regions of interest (ROIs) in four distinct axial slices of the liver. The following four axial MR elastogram slices were included for all patients: (i) slice including the left, middle, and right hepatic veins; (ii) slice including only the portal vein; (iii) slice in between the aforementioned two slices; (iv) slice inferior to slice (ii). ROIs likely to be influenced by artifacts were avoided. These ROIs include those in proximity to the falciform ligament, to large vessels, to the mechanical driver and chest wall, and to regions of highly variable stiffness. Custom MRE software was used to generate stiffness measurements in kiloPascals for these ROIs.

MRI-Guided Biopsy Technique

Real-time MRI-guided core needle biopsies of two separate Couinaud liver segments (one with the highest stiffness and one with lower) previously identified on MRE were obtained by attending interventional radiologists using MRI-compatible 18-gauge core needle devices (E-Z-EM, Inc, NY, USA). Biopsies were performed within the same MRI scanner as preceding MRE to facilitate direct correlation between MRE stiffness values and pathology specimens. Each patient was placed supine on the gantry table of the MRI scanner. Monitoring of blood pressure, oxygen saturation, and electrocardiography were performed during all procedures. The patient was anesthetized with local lidocaine and received intravenous moderate sedation with midazolam and fentanyl. The patient was prepped with a

sterile field above the liver span. Three fish oil tablets were placed along the span of the patient's liver. These served as surface fiducial markers for correlation with preliminary MRI to localize the insertion point of the biopsy needle. Preliminary hepatic MRI started with axial and coronal T2-weighted HASTE with parameters as follows: repetition time/ echo time, 1000 ms/85.0 ms; field of view, 400×400 mm^2; acquisition matrix, 166×256; slice thickness, 5 mm; bandwidth, 390 Hz/pixel; echo train length, 256; acquisition number, 1.

Axial T2-weighted interactive HASTE imaging was used to guide free-hand advancement of the needle toward the desired liver segment, while simultaneously observing needle position on an in-room monitor. Scan parameters were: repetition time/echo time, 2000-2500 ms/ 64.0 ms; field of view, 400×400 mm^2; acquisition matrix, 205×256; slice thickness, 5 mm; bandwidth, 390 Hz/pixel; echo train length, 256; acquisition number, 33. The interventional radiologist communicated image plane selection orally to the technologist in the control room via a two-way audio system. Needle advancement was stopped once the needle tip was within the liver segment targeted on MRE. Biopsies were acquired with 1-2 needle passes each from the highest and lower stiffness segments. Patients were monitored for 3-4 hours to ensure post-procedure clinical stability prior to discharge.

Liver Pathology Analysis

Core biopsy specimens were placed in separate containers of formalin and embedded them in paraffin. After staining with hematoxylin and eosin, periodic-acid Schiff, and/or Masson's trichrome, the specimens were assessed for METAVIR fibrosis stage (F0-F4) by an attending liver pathologist blinded to imaging findings. The METAVIR scoring system classifies hepatic fibrosis into five semiquantitative categories: F0-no fibrosis; F1-portal fibrosis without septa; F2-portal fibrosis and few septa extending into lobules; F3-numerous septa extending to adjacent portal tracts or terminal hepatic venules; and F4-cirrhosis (12). All specimens were further assessed for inflammation on a scale from 0 to 4. Hepatic inflammatory activity was classified into five semiquantitative categories: Grade 0-no portal inflammation; Grade 1-<50% portal tract with inflammatory infiltrate; Grade 2->50% portal tract with inflammatory infiltrate; Grade 3-above with interface hepatitis; and Grade 4-inflammatory infiltrate extending into lobule.

Data and Statistical Analysis

Pre-procedural liver function tests and MRI findings were initially recorded. The primary outcome measure was technical success, defined as the proportion of biopsies that resulted in specimens that could be graded for fibrosis and inflammation by the pathologist. Secondary outcome measures include a) the proportion of times that needle tip position could be detected in the targeted Couinaud segment with MRI; b) the frequency of patients experiencing post-procedural complications; and c) mean sedation time for the procedure. MRE stiffness values and fibrosis stages for the biopsied segments were determined in all patients and MRE stiffness values were compared between highest and lower stiffness segments using the Wilcoxon Signed Rank Test, with $\alpha = 0.05$. The mean overall liver MRE stiffness was also computed.

RESULTS

In all patients, diagnostic MRI revealed stable post-surgical changes related to liver transplantation. Technical success was achieved for all biopsy samples: 18/18 (100%) specimens were successfully graded for METAVIR fibrosis stage inflammatory grade. As secondary outcome measures, a) needle tip position could be detected during all 18 biopsies (100%); b) 1/9 patients (11%) experienced a minor complication (mild subcapsular bleeding

that required no further therapy); and c) mean procedural sedation time was 59 ± 24 min. A significant difference between the MRE value for the highest (4.61 ± 1.99 kPa; range, 2.07-7.60 kPa; median, 4.20 kPa) and lower (3.03 ± 1.75 kPa; range, 1.55-7.30 kPa; median, 2.67 kPa) stiffness biopsied segments (*P=0.0039*) was measured. All biopsies revealed stage F0 fibrosis on histopathology. 6 of 9 patients had Grade 1 inflammation in both specimens, while the remaining 3 patients had Grade 0 inflammation throughout their livers. The mean MRE stiffness measurement for the overall livers of the post-transplant patients was 3.14 ± 1.46 kPa (range, 2.00-6.80 kPa; median, 2.96 kPa). Table 1 lists patient characteristics, MRE stiffness values, and histopathology. Figure 1 and Figure 2 display sample imaging and pathology correlation. Table 2 shows pre-procedural liver function tests.

DISCUSSION

In this study, the use of MRI-guidance to obtain tissue specimens that could be directly correlated with segmental MRE values in post-liver transplant patients was introduced. Liver tissue specimens from all 9 patients were of sufficient quality to grade hepatic fibrosis and inflammation. As the needle tip could be visualized in the segment targeted with MRI for all biopsies, corresponding segmental MRE stiffness values could readily be generated. The results showed significant heterogeneity in MRE stiffness values within individual patients, and that MRI-guidance could successfully provide tissue samples from these heterogeneous regions. However, focal elevations in MRE stiffness were not associated with fibrosis on histopathology, as all biopsies yielded F0 staging.

The locally elevated values of liver stiffness identified in the absence of fibrosis [stage F0] may be due to inflammation and stellate cell activation (13). These findings are further supported by previous work with US-based transient elastography (TE) in post-transplant patients demonstrating increases in hepatic stiffness with the histologically assessed grade of necroinflammatory activity (14). Although overall liver MRE values correlate with hepatic fibrosis, recent evidence from Dr. Ehman's group demonstrates that MRE stiffness values are also elevated in the setting of inflammation prior to the onset of histological fibrosis in patients with nonalcoholic fatty liver disease (15). In their cohort, the mean MRE stiffness for patients with inflammation without fibrosis was 3.24 kPa. A study by Wang et al. showed a median MRE stiffness value of 3.32 kPA (interquartile range, 3.03-4.10 kPa) in patients with chronic hepatitis without fibrosis (16). Thus, studies in patients with non-alcoholic liver disease and with chronic hepatitis show MRE stiffness readings that are comparable to the 3.14 kPa mean value obtained in this study of post-transplant livers. Examination of inflammatory activity in our cohort revealed that 6 of 9 patients had mild hepatic inflammation in both specimens, while the remaining 3 of 9 patients lacked portal inflammation. No clear difference emerged regarding the degree of inflammation in the specimens obtained from high and low stiffness areas. This suggests that inflammatory activity may play a role in MRE stiffness reading elevation along with hepatic fibrosis but that stiffness readings in the post-transplant liver may be further influenced by other factors impacting tissue, including regional blood flow or local edema.

For HCV-positive patients, the standard of care is to perform annual or biennial liver biopsies after transplantation to monitor for histological recurrence (4). In the early stages of hepatic fibrosis, focal areas of liver fibrosis initially develop, which then gradually progress to more diffuse fibrosis, and ultimately cirrhosis. Histological recurrence indicates disease progression and influences the decision to initiate HCV therapy (4). Based on recent work by Lee et al., a cut-off of 3.81 kPa overall MRE stiffness in post-transplant livers has 87.5% sensitivity and 79.2% specificity for distinction of greater than stage 1 fibrosis (10). Real-time MRI-guided biopsies targeting segments of heterogeneous MRE-based stiffness, as performed in our study, may have the potential to enable earlier diagnosis of recurrence and

prompt initiation of treatment in post-transplant patients. Unlike previous studies validating MRE that have correlated with pathology results based on blind or US-guided percutaneous liver biopsies (9, 17), the technique of using real-time MRI additionally offers a functional guidance method that spatially co-localizes needle tip position with corresponding focal MRE stiffness. This method may validate the ability of MRE to assess segmental liver pathology in addition to the previously demonstrated ability to assess generalized liver pathology.

When seeking to correlate tissue specimens with MRE, there are several advantages of MRI- over US- and CT-guidance. Unlike US, MRI-guidance can depict final needle tip position in a format that is easily co-registered to corresponding areas on MRE. While MRI can display conventional planes and the entire liver span, US requires an "acoustic window" (18) that may not penetrate deep segments of liver, particularly in obese patients. US also contains more operator variability than MRI. Compared to CT, MRI avoids ionizing radiation and allows biopsies to be performed immediately after MRE without patient transfer.

MRE has technical advantages over other current techniques to non-invasively assess hepatic fibrosis. Other imaging techniques, including double contrast material-enhanced MRI, have shown promise only in the detection of advanced fibrosis (17, 19). In addition, although US-based TE has been reported to be a reliable method for diagnosing the development of fibrosis in liver transplant patients, this technology can only provide measurements of stiffness near the periphery of the liver and does not provide a global view of liver stiffness (9, 20). Using US-based TE, the risk of technical failure increases nine-fold among patients with central obesity (body mass index > 28 kg/m^2) (9, 20). MRE, in contrast, has been shown to be effective in detecting elevated liver stiffness measurements in patients with obesity or ascites and does not appear to demonstrate corresponding increased rates of technical failure (9).

There are several important limitations to this study. First, the sample size of 9 patients is too small to determine the diagnostic performance of MRE for detecting segmental liver fibrosis, and no clear trends emerged from the analysis of hepatic inflammation impacting MRE stiffness readings. Such assessments would require a future, larger prospective study. Second, long-term clinical and imaging follow-up on the cohort was not collected because the primary focus was to validate the technique of using MRI-guidance to biopsy segments of heterogeneous MRE liver stiffness. Finally, the acoustic drivers and analysis software required for MRE are not available for all commercial MRI scanners and are not currently FDA-approved.

In summary, real-time MRI guidance can be combined with MRE to target regions of heterogeneous liver stiffness in post-transplant patients. This study supports the use of MRI-guidance to sample tissue based upon functional information. The impact of this technique on clinical outcomes awaits verification from future studies.

Acknowledgments

References

1. Shepard CW, Finelli L, Alter MJ. Global epidemiology of hepatitis C virus infection. Lancet Infect Dis. 2005; 5:558–567. [PubMed: 16122679]

2. Mukherjee S, Sorrell MF. Controversies in liver transplantation for hepatitis C. Gastroenterology. 2008; 134:1777–1788. [PubMed: 18471554]

3. Gane E. The natural history and outcome of liver transplantation in hepatitis C virus-infected recipients. Liver Transpl. 2003; 9:S28–S34. [PubMed: 14586892]

4. Levitsky J, Doucette K. Viral hepatitis in solid organ transplant recipients. Am J Transplant. 2009; 9:S116–S130. [PubMed: 20070671]

5. Bravo AA, Sheth SG, Chopra S. Liver Biopsy. N Engl J Med. 2001; 344:495–500. [PubMed: 11172192]

6. Regev A, Berho M, Jeffers LJ, et al. Sampling error and intraobserver variation in liver biopsy in patients with chronic HCV infection. Am J Gastroenterol. 2002; 97:2614–2618. [PubMed: 12385448]

7. Schmidt AJ, Kee ST, Sze DY, et al. Diagnostic yield of MR-guided liver biopsies compared with CT- and US-guided liver biopsies. J Vasc Interv Radiol. 1999; 10:1323–1329. [PubMed: 10584646]

8. Muthupillai R, Lomas DJ, Rossman PJ, Greenleaf JF, Manduca A, Ehman RL. Magnetic resonance elastography by direct visualization of propagating acoustic strain waves. Science. 1995; 269:1854–1857. [PubMed: 7569924]

9. Yin M, Talwalkar JA, Glaser KJ, et al. Assessment of hepatic fibrosis with magnetic resonance elastography. Clin Gastroenterol Hepatol. 2007; 5:1207–1213. [PubMed: 17916548]

10. Lee VS, Miller FH, Omary RA, et al. Magnetic resonance elastography and biomarkers to assess fibrosis from recurrent hepatitis C in liver transplant recipients. Transplantation. 2011; 92:581–586. [PubMed: 21822174]

11. Manduca A, Oliphant TE, Dresner MA, et al. Magnetic resonance elastography: non-invasive mapping of tissue elasticity. Med Image Anal. 2001; 5:237–254. [PubMed: 11731304]

12. The French METAVIR Cooperative Study Group. Bedossa P. Intraobserver and interobserver variations in liver biopsy interpretation in patients with chronic hepatitis C. Hepatology. 1994; 20:15–20. [PubMed: 8020885]

13. Salameh N, Larrat B, Abarca-Quinones J, et al. Early detection of steatohepatitis in fatty rat liver by using MR elastography. Radiology. 2009; 253:90–97. [PubMed: 19587308]

14. Rigamonti C, Donato MF, Fraquelli M, et al. Transient elastography predicts fibrosis progression in patients with recurrent hepatitis C after liver transplantation. Gut. 2008; 57:821–827. [PubMed: 18218676]

15. Chen J, Talwalkar JA, Yin M, Glaser KJ, Sanderson SO, Ehman RL. Early detection of nonalcoholic steatohepatitis in patients with nonalcoholic fatty liver disease by using MR elastography. Radiology. 2011 [Epub ahead of print].

16. Wang Y, Ganger DR, Levitsky J, et al. Assessment of chronic hepatitis and fibrosis: Comparison of MR elastography and diffusion-weighted imaging. American Journal of Roentgenology. 2011; 196:553–561. [PubMed: 21343496]

17. Huwart L, Sempoux C, Salameh N, et al. Liver fibrosis: noninvasive assessment with MR elastography versus aspartate aminotransferase to-platelet ratio index. Radiology. 2007; 245:458–466. [PubMed: 17940304]

18. Rouviere O, Yin M, Dresner MA, et al. MR elastography of the liver: preliminary results. Radiology. 2006; 240:440–448. [PubMed: 16864671]

19. Aguirre DA, Behling CA, Alpert E, Hassanein TI, Sirlin CB. Liver fibrosis: noninvasive diagnosis with double contrast material-enhanced MR imaging. Radiology. 2006; 239:425–437. [PubMed: 16641352]

20. Foucher J, Castera L, Bernard P-Hb, et al. Prevalence and factors associated with failure of liver stiffness measurement using FibroScan in a prospective study of 2114 examinations. Eur J Gastroenterol Hepatol. 2006; 18:411–412. [PubMed: 16538113]
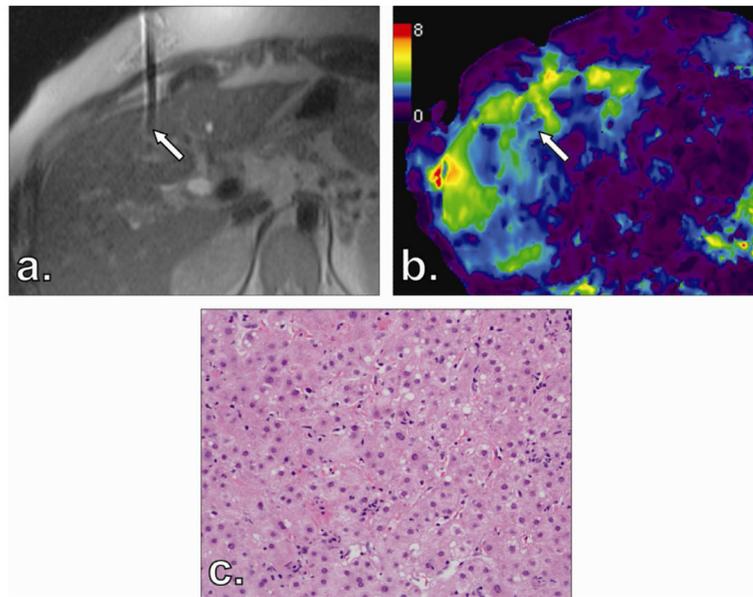
Figure 1.
Final needle tip position for Patient 7′s liver biopsy of segment 4 in T2-weighted half-Fourier acquisition single-shot turbo spin echo (HASTE) magnetic resonance imaging (MRI) **(a)** corresponds with magnetic resonance elastography (MRE) scan **(b)**. Corresponding specimen stained with hematoxylin and eosin reveals no fibrosis (stage F0) **(c)**.
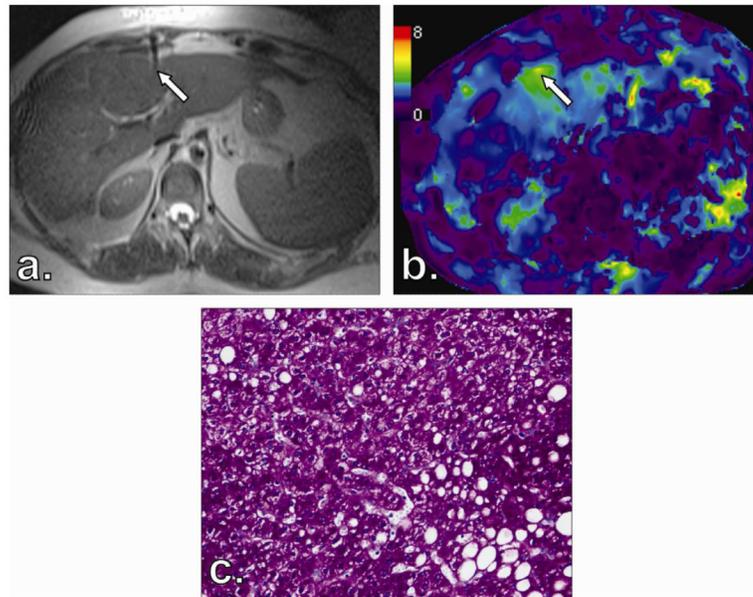
Figure 2.
Final needle tip position for Patient 1′s liver biopsy of segment 4 in T2-weighted HASTE
MRI **(a)** corresponds with magnetic resonance elastography (MRE) scan **(b)**. Corresponding
specimen stained with periodic-acid Schiff reveals no fibrosis (stage F0) **(c)**.

Table 1

Patient demographics, MRE findings, fibrosis score, and inflammation score.

Patient	Age	Sex	Overall MRE Stiffness (kPa)	Couinaud Liver Segment	Segmental MRE Stiffness (kPa)	Fibrosis Score (METAVIR scale)	Inflammation Score (Graded from 0-4)
1	55	Female	2.34	8	1.83	F0	1
1				4	2.85	F0	1
2	65	Female	2.34	7	2.30	F0	1
2				4	4.20	F0	1
3	54	Male	2.22	8	1.55	F0	1
3				4	2.96	F0	1
4	59	Male	2.96	8	3.35	F0	1
4				4	7.35	F0	1
5	60	Male	6.80	4	7.30	F0	0
5				8	7.60	F0	0
6	58	Male	2.00	8	1.73	F0	1
6				4	2.07	F0	1
7	42	Male	3.40	5	3.46	F0	1
7				4	5.24	F0	1
8	54	Male	3.01	5	2.67	F0	0
8				4	5.69	F0	0
9	59	Male	3.20	5	3.11	F0	0
9				4	3.52	F0	0

MRE, magnetic resonance elastography.

Table 2

Pre-procedural liver function tests.

Test	Mean and Range
AST (U/L)	45.9 (16-74)
ALT (U/L)	46.6 (13-97)
Total bilirubin (g/dL)	1.24 (0.6-3.3)
Alkaline phosphatase (U/L)	89.3 (43-141)
Albumin (g/dL)	3.97 (3.5-4.3)
Platelets (k/µL)	155 (79-225)
INR	0.978 (0.9-1.1)

AST, Aspartate aminotransferase; ALT, Alanine aminotransferase; INR, International normalized ratio.